Increasing Multiyear Sea Ice Loss in the Beaufort Sea: A New Export Pathway for the Diminishing Multiyear Ice Cover of the Arctic Ocean

David Gareth Babb[1], Ryan J. Galley[2], Stephen E. L. Howell[3], Jack Christopher Landy[4], Julienne Christine Stroeve[1], and David G. Barber[1]

[1]University of Manitoba
[2]Department of Fisheries and Oceans Canada
[3]Environment and Climate Change Canada
[4]University of Tromsø - The Artic University of Norway

November 24, 2022

Abstract

Historically multiyear sea ice (MYI) covered a majority of the Arctic and circulated through the Beaufort Gyre for years. However, increased ice melt in the Beaufort Sea during the early-2000s was proposed to have severed this circulation. Constructing a regional MYI budget from 1997-2021 reveals that MYI import into the Beaufort Sea has increased year-round, yet less MYI now survives through summer and is transported onwards in the Gyre. Annual average MYI loss quadrupled over the study period and increased from ~7% to ~33% of annual Fram Strait MYI export, while the peak in 2018 (385,000 km^2) was similar to Fram Strait MYI export. An accelerating ice-albedo feedback coupled with dynamic conditioning towards younger thinner MYI is responsible for the increased MYI loss. MYI transport through the Beaufort Gyre has not been severed, but it has been reduced so severely to prevent it from being redistributed throughout the Arctic Ocean

Increasing Multiyear Sea Ice Loss in the Beaufort Sea: A New Export Pathway for the Diminishing Multiyear Ice Cover of the Arctic Ocean

David G. Babb[1] (david.babb@umanitoba.ca) (ORCID: 0000- 0002-7427-8094)
Ryan J. Galley[2, 3] (ORCID: 0000-0002-5403-9694)
Stephen E.L. Howell[4] (ORCID: 0000-0002-4848-9867)
Jack C. Landy[5] (ORCID: 0000-0002-7372-1007)
Julienne C. Stroeve[1, 6, 7] (ORCID: 0000-0001-7316-8320)
David G. Barber[1] (ORCID: 0000-0001-9466-329)

[1] Centre for Earth Observation Science, University of Manitoba, Winnipeg, MB, Canada
[2] Department of Environment and Geography, University of Manitoba, Winnipeg, MB, Canada
[3] Department of Fisheries and Oceans Canada, Winnipeg, MB, Canada.
[4] Environment and Climate Change Canada, Toronto, ON, Canada
[5] Department of Physics and Technology, UiT The Arctic University of Norway, 9037 Tromsø, Norway;
[6] CPOM, London, United Kingdom
[7] NSIDC, Boulder, Colorado, United States

Keywords:

Sea ice; Multiyear ice; Beaufort Sea; Arctic Ocean; Sea ice dynamics; Beaufort Gyre

Key Points:

1. MYI area loss in the Beaufort Sea quadrupled from 46,000 km^2 yr^{-1} in 1997-2001 to 183,000 km^2 yr^{-1} in 2017-2021.

2. MYI area loss peaked at 385,000 km^2 in 2018, which is close to the annual MYI area export through Fram Strait.

3. The Beaufort Sea has become a MYI export pathway rivaling Fram Strait, encouraging the transition to a seasonal Arctic sea ice cover.

33   **Abstract:**

34   Historically multiyear sea ice (MYI) covered a majority of the Arctic and
35   circulated through the Beaufort Gyre for years. However, increased ice melt in the
36   Beaufort Sea during the early-2000s was proposed to have severed this circulation.
37   Constructing a regional MYI budget from 1997-2021 reveals that MYI import into
38   the Beaufort Sea has increased year-round, yet less MYI now survives through
39   summer and is transported onwards in the Gyre. Annual average MYI loss
40   quadrupled over the study period and increased from ~7% to ~33% of annual Fram
41   Strait MYI export, while the peak in 2018 (385,000 km^2) was similar to Fram Strait
42   MYI export. An accelerating ice-albedo feedback coupled with dynamic conditioning
43   towards younger thinner MYI is responsible for the increased MYI loss. MYI
44   transport through the Beaufort Gyre has not been severed, but it has been reduced
45   so severely to prevent it from being redistributed throughout the Arctic Ocean.

46

47   **Plain Language Summary:**

48   Historically sea ice grew thicker and aged into multiyear sea ice (MYI) as it
49   was transported clockwise around the Beaufort Gyre for up to and beyond 10 years.
50   This pattern facilitated the pan-Arctic distribution of MYI that was typical of the
51   1980s and 1990s. However, warming temperatures and greater sea ice melt in the
52   Beaufort Sea since the early 2000s has significantly increased the annual area of MYI
53   lost to melt, and was proposed to have severed MYI transport through the Beaufort
54   Gyre. Here we use a regional MYI budget to show that an increasing area of MYI is
55   lost annually in the Beaufort Sea and that this has considerably altered and
56   interrupted MYI transport through the Gyre for prolonged periods during recent
57   years. This change has implications regionally for wildlife, shipping, and local
58   communities, while also having an affect on the resiliency of the pan-Arctic ice pack.

1. Introduction:

Multiyear sea ice (MYI) comprises the thickest and most robust sea ice in the Arctic, however its extent is declining as the Arctic transitions to a predominantly seasonal ice cover (Kwok, 2018). Historically, MYI covered the vast majority of the Arctic (~5.5 x 10^6 km^2; Nghiem et al., 2007) and grew thicker as it circulated through the anticyclonic Beaufort Gyre for up to and beyond 10 years (Rigor & Wallace, 2004). In particular, years with a strong Beaufort Gyre (associated with the negative phase of the Arctic Oscillation (AO)) were generally conservative of MYI as they promoted MYI redistribution and limited ice export through Fram Strait (Rigor & Wallace, 2002; Stroeve et al., 2011). Within the Gyre, MYI is transported from the central Arctic, where the thickest and oldest ice is compressed against the northern coast of Greenland and the Canadian Arctic Archipelago (CAA; Bourke & Garret, 1987; Kwok, 2015), through the Beaufort Sea and on to the Eastern Arctic (Figure 1). The Beaufort Sea has therefore served as a conduit connecting the central Arctic to the Eastern Arctic and maintained the pan-Arctic distribution of MYI that was prevalent through the 1980s, 1990s and early 2000s (Maslanik et al., 2011). Critical to its role as a MYI conduit was the fact that from 1981-2005, 93% of MYI in the Beaufort Sea survived through summer (Maslanik et al., 2011).

Anomalous atmospheric forcing and record ice-loss during 1998 started the transition of the Beaufort ice pack to a thinner state (Hutchings & Rigor, 2012; Maslanik et al., 1999), and simultaneously sea ice melt, particularly bottom melt, increased in the early 2000s due to enhanced solar heating of the upper ocean (Perovich et al., 2008, 2011; Planck et al., 2020). In particular, Perovich et al., (2008) observed over 2 m of bottom melt on a 3 m thick MYI floe during summer 2007. This was six times greater than the mean value of bottom melt recorded in the 1990's and was attributed to anomalous solar heating of the upper ocean. Increased melt led to a reduction in MYI thickness from 2003-2012 (Krishfield et al., 2014), and an increase in MYI loss within the Beaufort Sea from 2000 through to a peak in 2008 (Kwok & Cunningham, 2010). Ultimately, the survival rate of MYI passing through the Beaufort Sea decreased to 73% from 2006-2010 (Maslanik et al., 2011), a change that was further emphasized by the complete loss of the regional MYI pack

90 during summers 2010, 2012 and 2016 (Babb et al., 2016, 2019; Stroeve et al., 2011).

91 However, regardless of MYI loss during summer, the Beaufort Sea has continued to

92 be resupplied with MYI from the central Arctic via the Gyre (Babb et al., 2020; Galley

93 et al., 2016; Howell et al., 2016), though less and less of it is likely to survive through

94 summer and as a result younger ice has been exported across the western gate of

95 the Beaufort Sea (Howell et al., 2016). This has led to younger ice recirculating

96 within the Gyre (Hutchings & Rigor, 2012) and all but eliminated the supply of MYI

97 to the Eastern Arctic which has been a predominantly seasonal ice cover since the

98 mid-2000s (Nghiem et al., 2006).

99   Based on the increase in MYI loss in the Beaufort Sea during the early-2000s

100 Maslanik et al. (2007) proposed that the previously continuous journey of MYI

101 through the Beaufort Gyre had been severed and that the western Arctic had

102 become an area of MYI export. In this paper we use 25 years of Canadian Ice Service

103 (CIS) ice charts to present a MYI budget for the Beaufort Sea that accounts for MYI

104 transport and quantifies the annual area of MYI lost to melt in the region from 1997

105 to 2021. We then examine the thermodynamic forcing and dynamic conditioning

106 that is driving the increase in MYI loss and examine MYI loss in the Beaufort Sea

107 relative to MYI export through other pathways. Ultimately, we examine whether

108 MYI transport through the Beaufort Gyre has been severed, leaving the Beaufort Sea
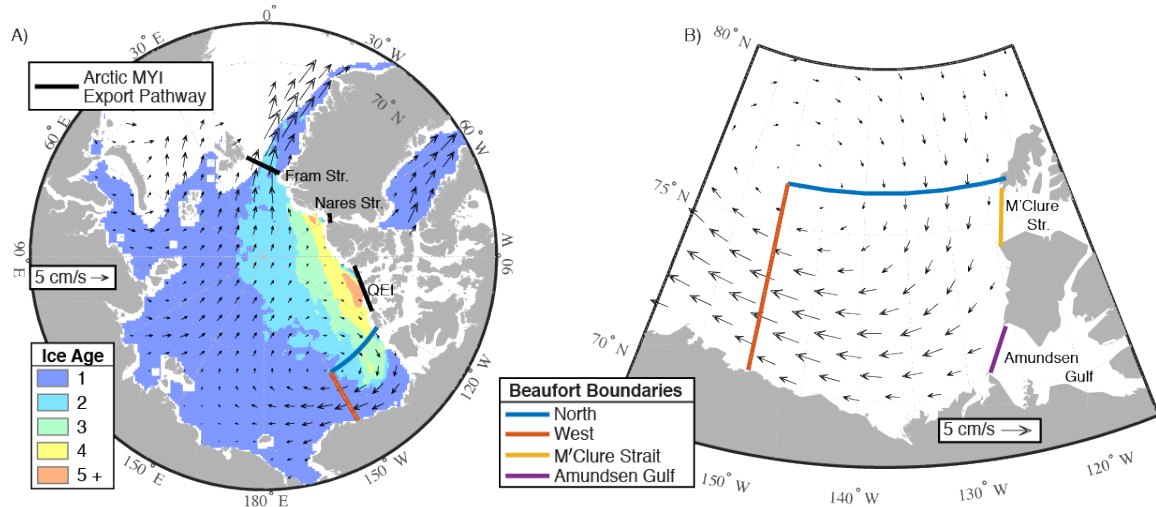
109 as an area of MYI export.

110

Figure 1: A) 1979-2020 mean field of sea ice motion and 2007-2020 median ice age at the end of April, with the northern and western bounds for the Beaufort Sea study region presented and the MYI export pathways marked. B) Close up of the mean field of sea ice motion through the Beaufort Sea, with the four boundaries of the Beaufort Sea study region presented. Ice Age in A) is from the NSIDC EASE-Grid Sea Ice Age v4 dataset (Tschudi et al., 2019a).

2. Methods:

To examine the MYI budget of the Beaufort Sea, the region was defined by western (150°W) and northern (76.25°N) boundaries, with two additional boundaries across Amundsen Gulf and M'Clure Strait (Figure 1B). The western and northern boundaries meet around the centre of the Beaufort Gyre, approximately enclosing its southeast quadrant (Figure 1A). The regional MYI area was calculated from weekly CIS digital ice charts and used to quantify the seasonal change in MYI area during summer (ΔMYI_S; May to the end of September) and winter (ΔMYI_W; October to the end of April). ΔMYI_W is solely the result of MYI transport across the boundaries, while a combination of MYI transport and melt dictate ΔMYI_S. Therefore, we estimate the annual area of MYI lost to melt by accounting for MYI transport. Beyond transport and melt, a small portion of MYI area may be reduced by compaction through ice deformation, however following Kwok and Cunningham (2010) this is expected to be very low and is not considered in this budget. Additionally, MYI forms locally during fall from FYI that survives through summer, which we do consider.

135   Ice charts delineate different ice regimes with polygons that present the
136   partial concentrations (tenths) of up to three different stages of development
137   according to the World Meteorological Organizations egg code (Fequet, 2005). Since
138   1996, ice charts are created by manually classifying these polygons in RADARSAT
139   images. Historically, the frequency of ice charts has varied between monthly, bi-
140   weekly and weekly intervals, though since 2007 ice charts have been produced
141   weekly year-round. Further details on the ice charts are discussed in Galley et al.,
142   (2016) and Tivy et al., (2011).

143   The seasonal MYI flux (F) was calculated across the western (F_W), northern
144   (F_N) and M'Clure (F_M) boundaries of the Beaufort Sea (Figure 1B). Amundsen Gulf
145   was not considered in the MYI flux calculations given that during our study period it
146   has been covered by a seasonal ice pack and the MYI pack within the Beaufort Sea
147   was typically located west of the gate (Galley et al., 2016). Daily values of F_W and F_N
148   were calculated at 5 km intervals across the gates:

$$F = c_{MYI}\, u\, \Delta x$$

150   where c_{MYI} is the MYI concentration at each point along the gate from the nearest ice
151   chart, u is the ice velocity component normal to the gate interpolated to each point,
152   and Δx is the distance between points (5 km). Ice velocity along the northern and
153   western gates was extracted from the Polar Pathfinder Daily 25 km EASE-Grid Sea
154   Ice Motion Vectors dataset (v4; Tschudi et al., 2019; updated 2021). However, the
155   dataset does not cover the narrow channels of the CAA, hence a finer resolution sea
156   ice motion dataset derived from sequential RADARSAT images (described in Howell
157   & Brady, 2019 and updated through 2021) was used in conjunction with the ice
158   charts to quantify monthly values of F_M. Note that F_M is null from November to April
159   as landfast ice conditions in M'Clure Strait impede ice motion (Canadian Ice Service,
160   2011). Across all three gates positive fluxes represent ice import, while negative
161   fluxes represent ice export from the Beaufort Sea. Cumulative seasonal ice fluxes are
162   calculated from 1 May to 30 September for summer, and from 1 October to 30 April
163   for winter. Lastly, the annual MYI area lost to melt is calculated as the difference
164   between ΔMYI_S and the net summer MYI flux across all three gates.

165   To compliment the MYI budget, several additional datasets were used. The

166   EASE-Grid Sea Ice Age dataset (Version 4 - Tschudi et al., 2019a) was used to

167   provide context on the age distribution of MYI within the Beaufort Sea at the end of

168   each winter. Unlike the CIS charts, which are manually created from RADARSAT

169   imagery, the ice age dataset tracks lagrangian parcels of sea ice through the Polar

170   Pathfinder ice motion dataset and counts how many years a parcel persists. The

171   Pan-Arctic Ice-Ocean Modelling and Assimilation System (PIOMAS; Zhang &

172   Rothrock, 2003) was used to provide estimates of ice thickness along the northern

173   and western boundaries of the Beaufort Sea. Additionally, six-hourly fields of 2 m air

174   temperature and surface solar radiation downwards (SSRD) were retrieved from

175   the ERA-5 reanalysis (Copernicus Climate Change Service (C3S), 2017). SSRD was

176   used in combination with daily fields of sea ice concentration (Cavalieri et al., 1996;

177   updated 2021) to estimate solar heating of the upper ocean through areas of open

178   water (F_{ow}) during summer:

179    $$F_{ow} = F_i(1 - \alpha) \, A_{ow}$$

180   where F_i is the daily sum of accumulated SSRD (J m^{-2}), α is the albedo of open water

181   (0.07) and A_{ow} is the area of open water. F_{ow} is strongly correlated with bottom melt

182   and has been associated with both the long-term increase in bottom melt and years

183   of anomalously high ice loss in the Beaufort Sea (Babb et al., 2016, 2019; Perovich et

184   al., 2008, 2011; Planck et al., 2020).

185

186   **3. Results and Discussion:**

187   **3.1 Regional MYI Budget**

188   From 1997 to 2021 there has been a significant negative trend in MYI area in

189   the Beaufort Sea at the start of May (-3,805 km^2 yr^{-1}) and end of September (-5,561

190   km^2 yr^{-1}; Figure 2A). The trend in September is ~35% greater than the trend in May;

191   highlighting the tendency towards greater reductions in MYI area during summer

192   and the continued replenishment of MYI during winter, which offsets MYI loss from

193   the previous summer (Figure 2B). This was exemplified during the winters of 2013

194   and 2018 following extreme summer ice loss. Other than import, MYI is replenished

195 by FYI surviving through summer, a process that has been fairly limited over this
196 25-year period (mean = 28,850 km^2) with the exception of 2013 (Figure 2B).

197   In terms of MYI transport, the net seasonal MYI flux varies considerably
198 between years according to the balance of western export and northern import,
199 with transport through M'Clure Strait accounting for only 10% of the summer MYI
200 flux (Figure 2). During winter the average net MYI flux is an export of 4,490 km^2, but
201 there is considerable interannual variability between import and export. For
202 example, the net winter export peaked at 245,000 km^2 in 1998 and preconditioned
203 the first regional sea ice minimum (Maslanik et al., 1999), while the net winter
204 import peaked at 183,500 km^2 in 2013 and replenished MYI in the Beaufort Sea
205 following the complete loss of the Beaufort ice pack in summer 2012 (Babb et al.,
206 2016; Figure 2C). Underlying the variability in MYI fluxes during winter there is a
207 significant positive trend in MYI import (+6,315 km^2 yr^{-1}) that has flipped winter
208 from a period of MYI export at the start of the time series to a period of MYI import
209 and replenishment more recently (Figure 2C).

210   During summer, an average of 47,120 km^2 of MYI is imported into the
211 Beaufort Sea (Figure 2D). Summer export peaked at 99,430 km^2 in 1997 and
212 contributed to the dramatic loss of MYI prior to the 1998 minimum, while net
213 summer import peaked at 312,670 km^2 in 2018, and was solely the result of
214 northern import. From 1997-2021, there has been a significant positive trend in
215 northern MYI import during summer (+5,071 km^2 yr^{-1}; Figure 2D).

216   Overall, from 1997-2021, MYI transport through the Beaufort Sea was highly
217 variable, but significant trends towards greater MYI import year-round have been
218 loading MYI from the central Arctic into the Beaufort. However, less of this MYI is
219 surviving through summer. From 1997-2021, an average of 125,000 km^2 of MYI
220 area was lost in the Beaufort Sea each summer. The minimum loss occurred in 2017,
221 when very little MYI was present in the Beaufort following the reversal of the
222 Beaufort Gyre (Babb et al., 2020), while the maximum loss (385,000 km^2) occurred
223 in 2018 (Figure 2E), though record northern import (Figure 2D) maintained a peak
224 in regional MYI area during September 2018 (Figure 2). Between 1997-2021 there
225 was a significant increase in MYI loss in the Beaufort Sea (-6,005 km^2 yr^{-1}; Figure

226   2E). The fact that the trend in MYI loss is similar to the trend in September MYI area

227   (-5,561 km^2 yr^{-1}), coupled with a non-significant trend in net MYI transport during

228   summer, indicates that melt, not transport, is driving the increased loss of MYI in the

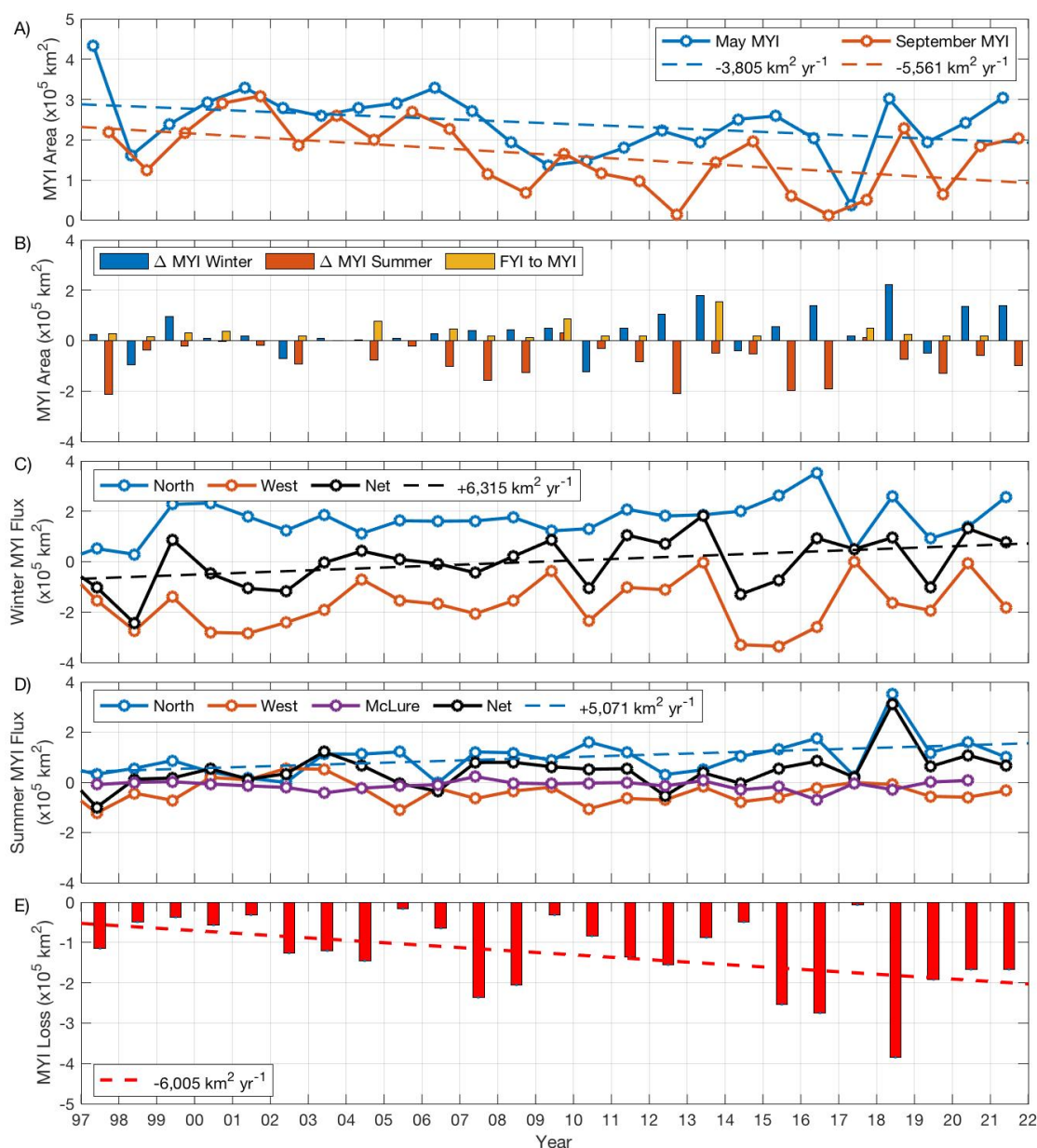229   Beaufort Sea during summer.

230
231   Figure 2: Annual time series of the MYI budget from 1997 to 2021. A) MYI area in
232   the Beaufort Sea during May (blue) and September (orange). B) Seasonal changes in
233   MYI area during winter (blue) and summer (orange), and the retention of FYI into
234   MYI during October (yellow). MYI fluxes during winter (C) and summer (D) across
235   the northern (blue), western (orange) and M'Clure (purple) gates, along with the net
236   seasonal MYI flux (black). E) MYI area loss in the Beaufort Sea. Dashed lines denote
237   significant (p < 0.05) trends.

238 **3.2 Thermodynamic forcing and dynamic conditioning of MYI loss**

239   MYI loss is not a new phenomenon in the Beaufort Sea; though between 1981
240 and 2005 only 7% of MYI in the western Arctic melted out each summer (Maslanik
241 et al., 2011). The recent increase in MYI loss reflects a balance of factors that either
242 drive ice melt (i.e. air temperatures, solar heating of the upper ocean) or dictate the
243 condition and therefore the resiliency of the ice pack entering the melt season (i.e.
244 thickness and age). Examining these factors over the same period as the budget
245 reveals non-significant increases in air temperatures and solar heating of the upper
246 ocean during summer, with notable peaks during years of regional sea ice minima
247 (1998, 2008, 2012 and 2016; Figure 3) during which MYI loss also peaked (Figure
248 2E). At the same time, the presence of MYI in the Beaufort Sea has not only declined,
249 but the age of the MYI has decreased, with a dramatic loss of MYI 5+ years old since
250 2010 (Figure 3C). This accompanies a significant negative trend in ice thickness
251 along the northern gate during both winter and summer (Figure 3d). Interestingly,
252 the peak in MYI loss during 2018 does not correspond to anomalously warm air
253 temperatures or greater solar heating of the upper ocean during summer, but rather
254 to an end of winter ice pack that was very young, with a majority of the MYI being
255 only 2 years old (Figure 3). Overall, the Beaufort ice pack has been progressively
256 conditioned towards a younger, thinner, less resilient state, while it has also been
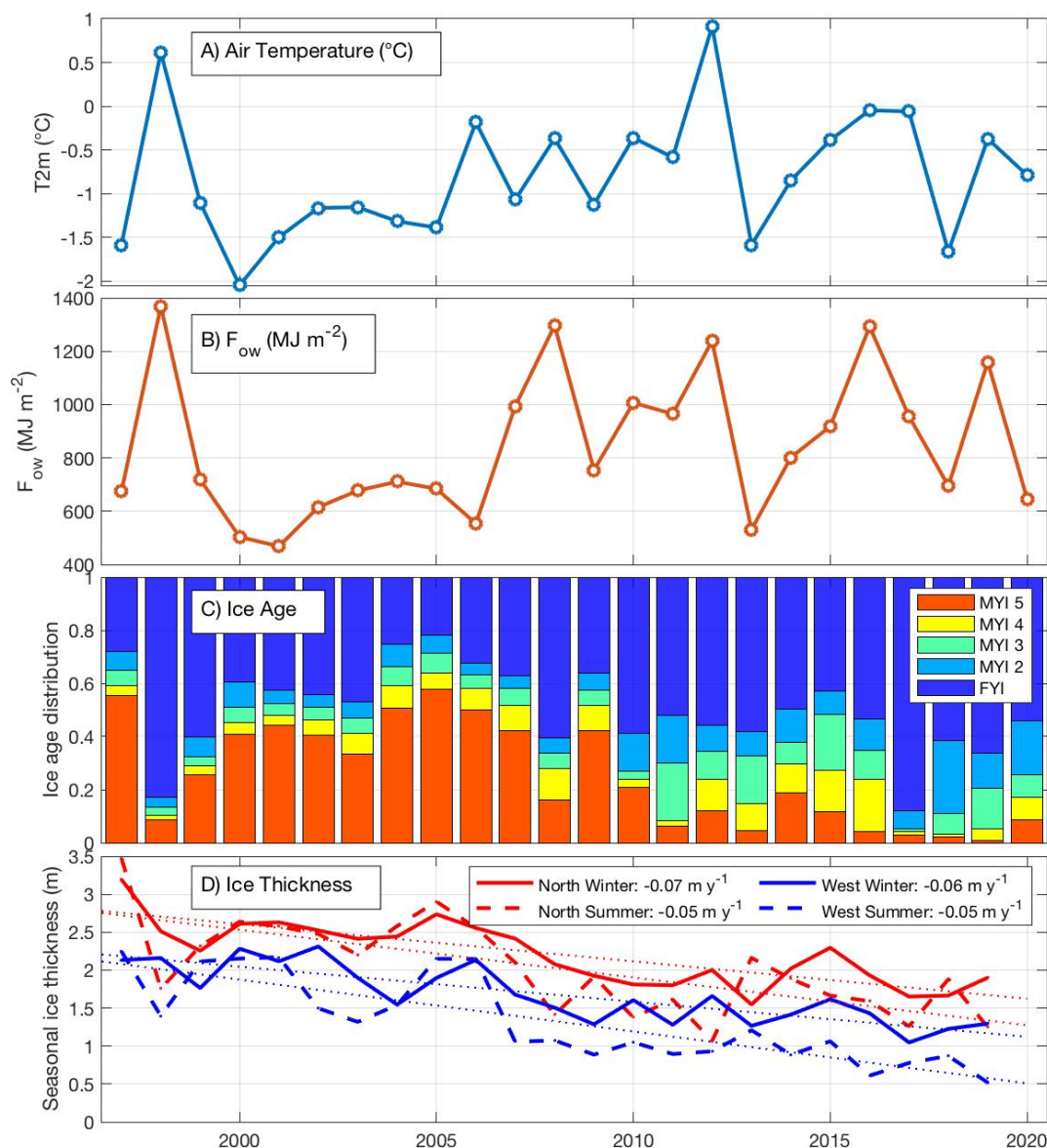257 exposed to warmer air temperatures and surface waters.

Figure 3: Time series of factors that either drive ice melt or condition the ice pack.
A) Mean 2 m air temperature over the Beaufort Sea from May through September.
B) Cumulative F_{ow} in the Beaufort Sea from May through September. C) Distribution
of ice age within the Beaufort Sea at the end of April. D) Mean seasonal ice thickness
along the northern (red) and western (blue) boundaries during winter (solid) and
summer (dashed) from PIOMAS. Significant trends ($p < 0.05$) are presented with
dotted lines.

3.3 Has MYI loss severed MYI transport within the Beaufort Gyre?

From 1997-2020, an average of 200,000 km² of MYI was exported from the
Beaufort Sea across the western gate annually. However, western export is highly
variable, and ranged from a maximum export of 406,000 km² in 2014 following the

271 recovery of MYI in 2013, to a net import of 750 km^2 in 2017 as a result of the

272 Beaufort Gyre reversal (Babb et al., 2020). Strong variability in MYI export

273 precludes significant trends, although during four recent winters essentially no MYI

274 was exported across the gate (2009, 2013, 2017 and 2020; Figure 2C). Furthermore,

275 there is a significant positive trend in FYI export across the western gate (+11,300

276 km^2 yr^{-1}), indicating younger ice is being exported into the Chukchi Sea in place of

277 MYI.

278 Whilst there has not been a significant trend in MYI export across the

279 western gate, there has been a decrease in the thickness and physical character of

280 MYI being exported across the gate. At the end of summer 2009 the remnant MYI in

281 the western Beaufort Sea was heavily deteriorated and isothermal (Barber et al.,

282 2009), while since 2007 remnant MYI has been so thin that by the end of the

283 following winter it is as thick as the surrounding FYI (Mahoney et al., 2019).

284 Furthermore, there is also significant negative trend in sea ice thickness along the

285 western gate during summer and winter (Figure 3).

286 MYI transport from the Beaufort Sea into the Chukchi Sea as part of the

287 Beaufort Gyre has not been totally severed. However, reductions in the area,

288 thickness and age of MYI transported through the Beaufort Sea into the Chukchi Sea

289 have created an ice pack in the Pacific sector of the Arctic that is less resilient to

290 warm pacific waters flowing through the Bering Strait (Woodgate et al., 2010) and

291 the subsequent ice-albedo feedback (Serreze et al., 2016) that are collectively

292 driving ice loss in this area.

293

294 **3.4 Has the Beaufort Sea become an area of MYI export?**

295 Traditionally, MYI export occurs along the boundaries of the Arctic Ocean

296 and represents the total loss of MYI. Fram Strait is the primary export pathway

297 (Kwok, 2009) exporting between 450,000 and 660,000 km^2 of MYI annually (Table

298 1). MYI is also exported annually through Nares Strait and into the QEI (Howell &

299 Brady, 2019; Kwok, 2005, 2006; Moore et al., 2021), and has occasionally been

300 exported into the Barents Sea (Kwok, 2004) and through the Bering Strait (Babb et

301 al., 2013). To define the Beaufort Sea as an export pathway similar to these other

302   locations the regional MYI pack would have to be completely lost. This has
303   happened three times during the last decade (2010, 2012, 2016), but as we have just
304   shown MYI, albeit a younger and thinner form of MYI does continue to be advected
305   downstream within the Gyre. Hence, the Beaufort Sea has not completely become an
306   export pathway, but it increasingly resembles one.

307   Comparing MYI loss in the Beaufort to MYI export through the traditional
308   export pathways reveals that during the first pentad of our budget (1997-2001) MYI
309   loss in the Beaufort was approximately twice the net MYI export through Nares
310   Strait and into the QEI, but only 6% to 9% of the MYI export through Fram Strait
311   (Table 1). Comparatively, during the most recent pentad (2017-2021) MYI loss in
312   the Beaufort Sea was approximately three times the net MYI export through Nares
313   Strait and into the QEI, and approximately 27% to 40% of the annual MYI export
314   through Fram Strait (Table 1). Furthermore, the 2018 peak in MYI loss (385,000
315   km^2) was close to the conservative estimate of MYI export through Fram Strait.

316   Without estimates of MYI loss in other regions it is not possible to compare
317   sub-regional MYI loss to the overall pan-Arctic annual MYI loss (melt + export).
318   Although this comparison shows that amongst these four pathways of MYI loss, the
319   Beaufort Sea continues to have the second greatest magnitude, and that its relative
320   contribution to the Arctic MYI balance has significantly increased. This increase is
321   critical for the MYI that remains along northern Greenland and the CAA, as it is now
322   bookended by Fram Strait and the Beaufort Sea (Figure 1A) and is susceptible to
323   being lost through either side. Historically, MYI advected from the central Arctic
324   through the Beaufort Gyre was conserved, particularly during years with a strong
325   Beaufort High (negative AO; Rigor & Wallace, 2002; Stroeve et al., 2011). However,
326   increasing ice melt in the Beaufort makes it unlikely that MYI advected out of the
327   Central Arctic will survive through the Beaufort Sea, or will be heavily deteriorated
328   by the time it reaches the Chukchi Sea, and thereby limits the potential of a strong
329   Beaufort High from facilitating the redistribution and recovery of MYI. As an
330   example, during winter 2021 a strong Beaufort High advected MYI out of the central
331   Arctic into the Beaufort Sea (Mallett et al., 2021), and while this facilitated a slight
332   recovery in the time series of the regional MYI area (Figure 2A), over 170,000 km^2

333   of this MYI was lost (Figure 2E) and we speculate that the remaining MYI
334   experienced considerable melt.

335   Ultimately, the combination of increasing MYI loss in the Beaufort Sea
336   (Figure 2E), increasing MYI export through Nares Strait (Moore et al., 2021) and
337   into the QEI (Howell & Brady, 2019), and continued MYI export through Fram Strait
338   is depleting the reservoir of MYI in the Arctic Ocean, a trend which is compounded
339   by a concomitant decrease in MYI replenishment by FYI (Kwok, 2007). The
340   imbalance between MYI loss and FYI replenishment is being amplified by increasing
341   MYI loss in the Beaufort Sea, and is driving the transition to a predominantly
342   seasonal ice cover that is inherently thinner and will eventually lead to the
343   occurrence of a seasonally ice-free Arctic around the middle of this century (SIMIP,
344   2020).

345

346   Table 1: Comparison of MYI loss in the Beaufort Sea to MYI export across the
347   boundaries of the Arctic Ocean.

	Years			Annual MYI loss
MYI loss in the Beaufort Sea	1997-2001			42,360 km²
	2017-2021			183,250 km²
Export Pathway	**Years**	**Annual ice export**	**Proportion MYI**	**Annual MYI loss**
Fram Strait	1979-2007	706,000 km² [a]	64-94% [b]	451,000 – 663,000 km²
Nares Strait	1996-2002	33,000 km² [c]	50% [c]	16,500 km²
	2019-2021	87,000 km² [d]	50% [c]	43,500 km²
QEI	1997-2002	8,000 km² [e]	100%*	8,000 km²
	1997-2018	25,000 km² [f]	100%*	25,000 km²

348   Notes: [a] – Kwok (2009); [b] – Ricker et al., (2018); [c] – Kwok, (2005); [d] – Moore et al.,
349   (2021); [e] – Kwok, (2006); [f] – Howell et al., (2019).
350   * Assumed based on the CIS ice charts.

351

352   **3.5 The impacts of increasing MYI loss in the Beaufort Sea**

353　　　　The loss of MYI has various impacts on the way that humans and wildlife
354　interact with the ice pack within the Beaufort Sea. Given its thickness, and strength,
355　MYI represents a considerable hazard to vessels operating in ice-covered waters.
356　The reduction in MYI area within the Beaufort Sea corresponds to an increase in
357　shipping activity (Pizzolato et al., 2016), particularly pleasure craft that are
358　accessing the Northwest Passage (Dawson et al., 2018). Shipping in the Beaufort Sea
359　is proposed to continue to increase as the shipping season length continues to
360　increase (Mudryk et al., 2021). However, the continued replenishment of MYI during
361　winter will maintain some level of risk associated with hazardous ice (Barber et al.,
362　2014).

363　　　　The transition to a thinner seasonal ice pack is projected to increase
364　productivity in the Arctic (Tedesco et al., 2019) and has been proposed to offer
365　some short-term benefits to Polar Bears (Derocher et al., 2004). However, Laidre et
366　al., (2020) noted that this has yet to be demonstrated and suggest any advantage
367　may only be temporary before the negative effects of climate change (i.e. habitat
368　loss) begin to outweigh any potential positives. Historically, Polar Bears within the
369　Beaufort Sea retreated to the MYI pack during summer (Derocher et al., 2004) and
370　even denned on MYI floes during winter (Amstrup & Gardner, 1994). But MYI loss
371　(Figure 2E) combined with the northern retreat of the MYI edge (Galley et al., 2016),
372　is both removing and fragmenting this habitat and increasing the distance that bears
373　may need to swim to reach either the remaining MYI or land (Pagano et al., 2021).

374

375　**4. Conclusions:**

376　　　　Historically, the Beaufort Sea served as a conduit for MYI transport from the
377　central Arctic to the Eastern Arctic through the Beaufort Gyre, and thereby
378　facilitated the presence of MYI throughout much of the Arctic Ocean. However,
379　increasing ice melt during the early-2000s led Maslanik et al. (2007) to propose that
380　the Beaufort Sea had become an area of MYI export and that MYI transport through
381　the Beaufort Gyre had been severed. Using a regional MYI budget from 1997-2021,
382　we have determined that MYI transport through the Beaufort Sea has not been
383　completely severed, but that it has been interrupted and essentially now provides

384   no replenishment of MYI to the Eastern Arctic. The budget reveals that MYI import

385   into the Beaufort Sea has increased during both summer and winter, but that less of

386   this MYI now survives through summer. Over the 25-year study period, MYI area

387   loss increased at 6,289 km^2 yr^{-1}, nearly quadrupling the annual mean area of MYI

388   lost from 42,360 km^2 between 1997-2001 to 183,000 km^2 between 2017-2021. MYI

389   area loss peaked at 385,000 km^2 in 2018.

390   Historically, the pan-Arctic MYI budget was dominated by MYI loss through

391   Fram Strait. At the start of the record, MYI loss in the Beaufort Sea represented only

392   7% of the annual MYI export through Fram Strait. However, from 2017-2021 this

393   increased to ~35%, with the peak in 2018 matching the conservative estimate of

394   MYI export through Fram Strait (~400,000 km^2). This increase in MYI loss in the

395   Beaufort Sea has been driven by a combination of thermodynamic forcing and

396   dynamic conditioning, which have collectively exposed a younger, thinner ice pack

397   to warmer air temperatures and a warmer ocean. Increased MYI loss has

398   interrupted MYI transport through the Gyre, leading to a deteriorated form of MYI

399   being advected downstream and thereby affecting the state of the Chukchi Sea ice

400   pack. Ultimately, the contribution of MYI loss in the Beaufort Sea to the overall MYI

401   budget of the Arctic Ocean has dramatically increased and is a key driver of the

402   transition to a seasonal Arctic ice pack.

415

416 **Data Availability**

417 CIS ice charts are freely available online (https://www.canada.ca/en/environment-

418 climate-change/services/ice-forecasts-observations.html). The NSIDC ice motion

419 (https://nsidc.org/data/nsidc-0116/versions/4) and ice age

420 (https://nsidc.org/data/NSIDC-0611/versions/4) datasets are available online.

421 PIOMAS Ice thickness data is available online

422 (http://psc.apl.uw.edu/research/projects/arctic-sea-ice-volume-

423 anomaly/data/model_grid). ERA5 atmospheric reanalysis products are available

424 from the Climate Data Store through the Copernicus Climate Change Service

425 (https://cds.climate.copernicus.eu/cdsapp#!/dataset/reanalysis-era5-single-

426 levels?tab=overview).

427   **References:**

428   Amstrup, S. C., & Gardner, C. L. (1994). Polar bear maternity denning in the Beaufort
429   Sea. *Journal of Wildlife Management*, *58*(1), 1–10.
430   https://doi.org/10.2307/3809542
431   Babb, D.G., Landy, J. C., Lukovich, J. V., Haas, C., Hendricks, S., Barber, D. G., & Galley,
432   R. J. (2020). The 2017 reversal of the Beaufort Gyre: Can dynamic thickening of
433   a seasonal ice cover during a reversal limit summer ice melt in the Beaufort
434   Sea? *Journal of Geophysical Research: Oceans*, 1–26.
435   https://doi.org/10.1029/2020jc016796
436   Babb, David G., Galley, R. J., Asplin, M. G., Lukovich, J. V., & Barber, D. G. (2013).
437   Multiyear sea ice export through the Bering Strait during winter 2011-2012.
438   *Journal of Geophysical Research: Oceans*, *118*(10), 5489–5503.
439   https://doi.org/10.1002/jgrc.20383
440   Babb, David G., Galley, R. J., Barber, D. G., & Rysgaard, S. (2016). Physical processes
441   contributing to an ice free Beaufort Sea during September 2012. *Journal of
442   Geophysical Research: Oceans*, *121*, 267–283.
443   https://doi.org/10.1002/2015JC010756
444   Babb, David G., Landy, J. C., Barber, D. G., & Galley, R. J. (2019). Winter Sea Ice Export
445   From the Beaufort Sea as a Preconditioning Mechanism for Enhanced Summer
446   Melt: A Case Study of 2016. *Journal of Geophysical Research: Oceans*,
447   *1998*(6575), 6575–6600. https://doi.org/10.1029/2019JC015053
448   Barber, D. G., Galley, R. J., Asplin, M. G., De Abreu, R., Warner, K. A., Pučko, M., et al.
449   (2009). Perennial pack ice in the southern beaufort sea was not as it appeared
450   in the summer of 2009. *Geophysical Research Letters*, *36*(24), 1–5.
451   https://doi.org/10.1029/2009GL041434
452   Barber, D. G., McCullough, G., Babb, D. G., Komarov, A., Candlish, L. M., Lukovich, J. V.,
453   et al. (2014). Climate change and ice hazards in the Beaufort Sea. *Elementa:
454   Science of the Anthropocene*, *2*(1982), 000025.
455   https://doi.org/10.12952/journal.elementa.000025
456   Bourke, R. H., & Garret, R. P. (1987). Sea ice thickness distribution in the Arctic
457   Ocean. *Cold Regions Science and Technology*, *13*, 259–280.
458   Canadian Ice Service. (2011). *Sea Ice Climatic Atlas for the Northern Canadian Waters
459   1981-2011*. Ottawa, Canada.
460   Cavalieri, D. J., Parkinson, C. L., Gloersen, P., & Zwally, H. J. (1996). *Sea Ice
461   Concentrations from Nimbus-7 SMMR and DMSP SSM/I-SSMIS PAssive Microwave
462   Data*. Boulder, Colorado, USA.
463   Copernicus Climate Change Service (C3S). (2017). ERA5: Fifth generation of ECMWF
464   atmospheric reanalysis of the global climate. Copernicus Climate Change
465   Service Climate Data Store.
466   Dawson, J., Pizzolato, L., Howell, S. E. L., Copland, L., & Johnston, M. E. (2018).
467   Temporal and Spatial Patterns of Ship Traffic in the Canadian Arctic from 1990
468   to 2015 + Supplementary Appendix 1: Figs. S1–S7 (See Article Tools). *Arctic*,
469   *71*(1), 15. https://doi.org/10.14430/arctic4698
470   Derocher, A. E., Lunn, N. J., & Stirling, I. (2004). Polar Bears in a Warming Climate.
471   *Integrative and Comparative Biology*, *44*(2), 163–176.

472   https://doi.org/10.1093/icb/44.2.163

473   Fequet, D. (2005). *Manual of Standard Procedures for Observing and Reporting Ice*
474   *Conditions* (9th ed.). Ottawa: Canadian Ice Service, Environment Canada.

475   Galley, R. J., Babb, D. G., Ogi, M., Else, B. G. T., Geifus, N. X., Crabeck, O., et al. (2016).
476   Replacement of multiyear sea ice and changes in the open water season
477   duration in the Beaufort Sea since 2004. *Journal of Geophysical Research:*
478   *Oceans*, *121*(April), 1–18. https://doi.org/10.1002/2015JC011583.Received

479   Howell, S. E. L., & Brady, M. (2019). The Dynamic Response of Sea Ice to Warming in
480   the Canadian Arctic Archipelago. *Geophysical Research Letters*, *46*(22), 13119–
481   13125. https://doi.org/10.1029/2019GL085116

482   Howell, S. E. L., Brady, M., Derksen, C., & Kelly, R. E. J. (2016). Recent changes in sea
483   ice area flux through the Beaufort Sea during the summer. *Journal of*
484   *Geophysical Research: Oceans*, *121*, 1–14.
485   https://doi.org/10.1002/2015JC011464

486   Hutchings, J. K., & Rigor, I. G. (2012). Role of ice dynamics in anomalous ice
487   conditions in the Beaufort Sea during 2006 and 2007. *Journal of Geophysical*
488   *Research: Oceans*, *117*(5), 1–14. https://doi.org/10.1029/2011JC007182

489   Krishfield, R. A., Proshutinsky, A., Tateyama, K., Williams, W. J., Carmack, E. C.,
490   McLaughlin, F. A., & Timmermans, M.-L. (2014). Deterioration of perennial sea
491   ice in the Beaufort Gyre from 2003 to 2012 and its impact on the oceanic
492   freshwater cycle. *Journal of Geophysical Research: Oceans*, *119*, 35.
493   https://doi.org/10.1002/2013JC008999

494   Kwok, R. (2004). Fram Strait sea ice outflow. *Journal of Geophysical Research*,
495   *109*(C1), C01009. https://doi.org/10.1029/2003JC001785

496   Kwok, R. (2005). Variability of Nares Strait ice flux. *Geophysical Research Letters*,
497   *32*(24), 1–4. https://doi.org/10.1029/2005GL024768

498   Kwok, R. (2006). Exchange of sea ice between the Arctic Ocean and the Canadian
499   Arctic Archipelago. *Geophysical Research Letters*, *33*(16), 1–5.
500   https://doi.org/10.1029/2006GL027094

501   Kwok, R. (2007). Near zero replenishment of the Arctic multiyear sea ice cover at
502   the end of 2005 summer. *Geophysical Research Letters*, *34*(5), 1–6.
503   https://doi.org/10.1029/2006GL028737

504   Kwok, R. (2009). Outflow of Arctic Ocean sea ice into the Greenland and Barent Seas:
505   1979-2007. *Journal of Climate*, *22*(9), 2438–2457.
506   https://doi.org/10.1175/2008JCLI2819.1

507   Kwok, R. (2015). Sea ice convergance along the Arctic coasts of Greenland and the
508   Canadian Arctic Archipelago: Variability and extremes (1992-2014).
509   *Geophysical Research Letters*, *42*, 1–8. https://doi.org/10.1002/2015GL065462

510   Kwok, R. (2018). Arctic sea ice thickness, volume , and multiyear ice coverage: losses
511   and coupled variability (1958 – 2018). *Environmental Research Letters*, *13*(10),
512   105005. https://doi.org/10.1088/1748-9326/aae3ec

513   Kwok, R., & Cunningham, G. F. (2010). Contribution of melt in the Beaufort Sea to the
514   decline in Arctic multiyear sea ice coverage: 1993-2009. *Geophysical Research*
515   *Letters*, *37*(20), 1–5. https://doi.org/10.1029/2010GL044678

516   Laidre, K. L., Atkinson, S. N., Regehr, E. V, Stern, H. L., Born, E. W., Wiig, Ø., et al.
517   (2020). Transient benefits of climate change for a high-Arctic polar bear (Ursus

518   maritimus) subpopulation. *Global Change Biology*, *26*(11), 6251–6265.
519   https://doi.org/https://doi.org/10.1111/gcb.15286
520 Mahoney, A. R., Hutchings, J. K., Eicken, H., & Haas, C. (2019). Changes in the
521   Thickness and Circulation of Multiyear Ice in the Beaufort Gyre Determined
522   From Pseudo-Lagrangian Methods from 2003–2015. *Journal of Geophysical*
523   *Research: Oceans*, *124*(8), 5618–5633. https://doi.org/10.1029/2018JC014911
524 Mallett, R. D. C., Stroeve, J. C., Cornish, S. B., Crawford, A. D., Lukovich, J. V., Serreze,
525   M. C., et al. (2021). Record winter winds in 2020/21 drove exceptional Arctic
526   sea ice transport. *Communications Earth & Environment*, *2*(1), 17–22.
527   https://doi.org/10.1038/s43247-021-00221-8
528 Maslanik, J. A., Serreze, M. C., & Agnew, T. (1999). On the record reduction in 1998
529   Western Arctic sea-ice cover. *Geophysical Research Letters*, *26*(13), 1905–1908.
530   https://doi.org/10.1029/1999GL900426
531 Maslanik, J. A., Fowler, C., Stroeve, J. C., Drobot, S., Zwally, J., Yi, D., & Emery, W.
532   (2007). A younger, thinner Arctic ice cover: Increased potential for rapid,
533   extensive sea-ice loss. *Geophysical Research Letters*, *34*(24), 2004–2008.
534   https://doi.org/10.1029/2007GL032043
535 Maslanik, J. A., Stroeve, J. C., Fowler, C., & Emery, W. (2011). Distribution and trends
536   in Arctic sea ice age through spring 2011. *Geophysical Research Letters*, *38*(13),
537   2–7. https://doi.org/10.1029/2011GL047735
538 Moore, G. W. K., Howell, S. E. L., Brady, M., Xu, X., & McNeil, K. (2021). Anomalous
539   collapses of Nares Strait ice arches leads to enhanced export of Arctic sea ice.
540   *Nature Communications*, *12*(1), 1–8. https://doi.org/10.1038/s41467-020-
541   20314-w
542 Mudryk, L. R., Dawson, J., Howell, S. E. L., Derksen, C., Zagon, T. A., & Brady, M.
543   (2021). Impact of 1, 2 and 4 °C of global warming on ship navigation in the
544   Canadian Arctic. *Nature Climate Change*, 29–31.
545   https://doi.org/10.1038/s41558-021-01087-6
546 Nghiem, S. V., Chao, Y., Neumann, G., Li, P., Perovich, D. K., Street, T., & Clemente-
547   Colón, P. (2006). Depletion of perennial sea ice in the East Arctic Ocean.
548   *Geophysical Research Letters*, *33*(17), 1–6.
549   https://doi.org/10.1029/2006GL027198
550 Nghiem, S. V., Rigor, I. G., Perovich, D. K., Clemente-Colón, P., Weatherly, J. W., &
551   Neumann, G. (2007). Rapid reduction of Arctic perennial sea ice. *Geophysical*
552   *Research Letters*, *34*(19), 1–6. https://doi.org/10.1029/2007GL031138
553 Pagano, A. M., Durner, G. M., Atwood, T. C., & Douglas, D. C. (2021). Effects of sea ice
554   decline and summer land use on polar bear home range size in the Beaufort
555   Sea. *Ecosphere*, *12*(10). https://doi.org/10.1002/ecs2.3768
556 Perovich, D. K., Richeter-Menge, J. A., Jones, K. F., & Light, B. (2008). Sunlight, water,
557   and ice: Extreme Arctic sea ice melt during the summer of 2007. *Geophysical*
558   *Research Letters*, *35*(11), 2–5. https://doi.org/10.1029/2008GL034007
559 Perovich, D. K., Richter-Menge, J. A., Jones, K. F., Light, B., Elder, B. C., Polashenski, C.,
560   et al. (2011). Arctic sea-ice melt in 2008 and the role of solar heating. *Annals of*
561   *Glaciology*, *52*(57 PART 2), 355–359.
562   https://doi.org/10.3189/172756411795931714
563 Pizzolato, L., Howell, S. E. L., Dawson, J., Laliberté, F., & Copland, L. (2016). The

564 influence of declining sea ice on shipping activity in the Canadian Arctic.
565 *Geophysical Research Letters*, *43*(23), 12,146-12,154.
566 https://doi.org/10.1002/2016GL071489
567 Planck, C. J., Perovich, D. K., & Light, B. (2020). A Synthesis of Observations and
568 Models to Assess the Time Series of Sea Ice Mass Balance in the Beaufort Sea.
569 *Journal of Geophysical Research: Oceans*, 1–15.
570 https://doi.org/10.1029/2019jc015833
571 Ricker, R., Girard-Ardhuin, F., Krumpen, T., & Lique, C. (2018). Satellite-derived sea
572 ice export and its impact on Arctic ice mass balance. *The Cryosphere*, *12*(9),
573 3017–3032. https://doi.org/10.5194/tc-12-3017-2018
574 Rigor, I. G., & Wallace, J. M. (2002). Response of sea ice to the Arctic Oscillation.
575 *Applied Physics*, 2648–2663. https://doi.org/10.1175/1520-
576 0442(2002)015<2648:ROSITT>2.0.CO;2
577 Rigor, I. G., & Wallace, J. M. (2004). Variations in the age of Arctic sea-ice and
578 summer sea-ice extent. *Geophysical Research Letters*, *31*(9), 2–5.
579 https://doi.org/10.1029/2004GL019492
580 Serreze, M. C., Crawford, A. D., Stroeve, J. C., Barrett, A. P., & Woodgate, R. A. (2016).
581 Variability, trends, and predictability of seasonal sea ice retreat and advance in
582 the Chukchi Sea. *Journal of Geophysical Research: Oceans*, *121*, 7308–7325.
583 https://doi.org/10.1002/2016JC011977
584 SIMIP Community. (2020). Arctic Sea Ice in CMIP6. *Geophysical Research Letters*,
585 *47*(10). https://doi.org/10.1029/2019gl086749
586 Stroeve, J. C., Maslanik, J. A., Serreze, M. C., Rigor, I. G., Meier, W., & Fowler, C. (2011).
587 Sea ice response to an extreme negative phase of the Arctic Oscillation during
588 winter 2009/2010. *Geophysical Research Letters*, *38*(2), 1–6.
589 https://doi.org/10.1029/2010GL045662
590 Tedesco, L., Vichi, M., & Scoccimarro, E. (2019). Sea-ice algal phenology in a warmer
591 Arctic. *Science Advances*, *5*(5). https://doi.org/10.1126/sciadv.aav4830
592 Tivy, A., Howell, S. E. L., Alt, B., McCourt, S., Chagnon, R., Crocker, G., et al. (2011).
593 Trends and variability in summer sea ice cover in the Canadian Arctic based on
594 the Canadian Ice Service Digital Archive, 1960-2008 and 1968-2008. *Journal of
595 Geophysical Research: Oceans*, *116*(3). https://doi.org/10.1029/2009JC005855
596 Tschudi, M. A., Meier, W. N., Stewart, J. S., Fowler, C., & Maslanik, J. A. (2019a). *EASE-
597 Grid Sea Ice Age, Version 4*. Boulder, Colorado, USA.
598 https://doi.org/https://doi.org/10.5067/UTAV7490FEPB
599 Tschudi, M. A., Meier, W. N., Stewart, J. S., Fowler, C., & Maslanik, J. A. (2019b). *Polar
600 Pathfinder Daily 25 km EASE-Grid Sea Ice Motion Vectors, Version 4*. Boulder,
601 Colorado, USA. https://doi.org/https://doi.org/10.5067/INAWUWO7QH7B
602 Woodgate, R. A., Weingartner, T., & Lindsay, R. (2010). The 2007 Bering Strait
603 oceanic heat flux and anomalous Arctic sea-ice retreat. *Geophysical Research
604 Letters*, *37*(1), 1–5. https://doi.org/10.1029/2009GL041621
605 Zhang, J., & Rothrock, D. A. (2003). Modeling global sea ice with a thickness and
606 enthalpy distribution model in generalized curvilinear coordinates. *Monthly
607 Weather Review*, *131*(5), 845–861. https://doi.org/10.1175/1520-
608 0493(2003)131<0845:MGSIWA>2.0.CO;2
609